Fabrication and Characterization of Porous Membranes with Highly Ordered Three-Dimensional Periodic Structures

Byron Gates, Yadong Yin, and Younan Xia*

Department of Chemistry, University of Washington, Seattle, Washington 98195-1700

Received April 7, 1999. Revised Manuscript Received August 13, 1999

This paper describes a procedure that uses opaline arrays of spherical particles (with diameters ≥100 nm) as templates to fabricate porous membranes having three-dimensional interconnected networks of air balls. An aqueous dispersion of monodispersed polystyrene (or silica) beads was injected into a specially designed cell and assembled into an opaline array under external gas pressure and sonication. After drying, the void spaces among the spheres were filled with a liquid precursor such as a UV-curable (or thermally cross-linkable) prepolymer or a sol−gel solution. Subsequent solidification of the precursor and dissolution of the particles produced a well-defined porous membrane having a complex, three-dimensional architecture of air balls interconnected by a number of small circular "windows". The porous structure of this kind of membrane can be easily tailored by using colloidal particles with different sizes: when spherical particles of diameter *D* are used, the dimension of air balls in the bulk is ∼*D*, the size of circular windows interconnecting these air balls is ∼*D*/4, and the diameter of circular holes on the surfaces of the membrane is ∼*D*/2. We have demonstrated the fabrication procedure using a variety of materials, including a UV-curable poly(acrylate−methacrylate) copolymer (PAMC), UV-curable polyurethanes, and sol−gel precursors to oxide ceramics such as SiO_2 or TiO_2. The permeabilities of these porous membrane films for a number of commonly used solvents were tested with a PAMC membrane as the example. Our measurements indicate that the liquid permeability of this porous membrane strongly depends on the properties of the liquid. In addition to their uses in filtration, separation, and tissue engineering, the porous membranes described in this paper should also find applications in fabricating diffractive sensors and photonic band gap (PBG) materials due to their three-dimensional periodic structures.

Introduction

According to their pore sizes, the International Union of Pure and Applied Chemists (IUPAC) has recommended a specific nomenclature for porous materials: microporous (pore diameter <2 nm), mesoporous (2 nm < pore diameter <50 nm), and macroporous (pore diameter >50 nm).[1] Liquids and gases have been found to exhibit a characteristic transport behavior in each type of porous material: the dominant transport processes are viscous flow and molecular diffusion in a macroporous material, surface diffusion and capillary transport in a mesoporous material, and activated transport in a microporous material. Porous materials are useful in a wide range of applications: for example, as membranes for separation and purification,[2] as high surface area adsorbants,[3] as solid supports for sensors and catalysts,[4] as scaffolds for tissue engineering,[5] and as low-dielectric constant materials for microelectronic devices.[6] These materials have also been actively explored as photonic band gap (PBG) materials for use in optoelectronics[7] and as new types of mechanical materials that may exhibit negative Poisson ratios.[8]

Although a number of methods have been developed for generating porous materials,[1,2] it still remains a great challenge in fabricating three-dimensional (3D) porous membranes that have well-defined structures—precisely controlled pore sizes, fully exposed (on the surfaces) and completely interconnected (in the bulk) pores, and highly ordered periodic structures. Conventional methods based on electrochemical etching of alumina or silicon,[9] chemical etching of glasses,[10] ion-

* To whom correspondence should be addressed. E-mail: xia@chem.washington.edu.

(1) Schaefer, D. W. *MRS Bull.* **1994**, *19* (4), 14−17.
(2) Bhave, R. R. *Inorganic Membranes: Synthesis, Characteristics and Applications*; Van Nostrand Reinhold: New York, 1991.
(3) Fain, D. E. *MRS Bull.* **1994**, *19* (4), 40−43.
(4) (a) Keizer, K.; Verweij, H. *CHEMTECH* **1996**, *January*, 37−41. (b) Lin, V. S.-Y.; Motesharei, K.; Dancil, K. P. S.; Sailor, M. J.; Ghadiri, M. R. *Science* **1997**, *278*, 840−843.
(5) Hubbell, J. A.; Langer, R. *Chem. Eng. News* **1995**, *March 13*, 42.
(6) (a) Prakash, S. S.; Brinker, C. J.; Hurd, A. J.; Rao, S. M. *Nature* **1995**, *374*, 439−443. (b) Hedrick, J. L.; Miller, R. D.; Hawker, C. J.; Carter, K. R.; Volksen, W.; Yoon, D. Y.; Trollsås, M. *Adv. Mater.* **1998**, *10*, 1049−1053.
(7) See, for example, Joannopoulos, J. D.; Villeneuve, P. R.; Fan, S. *Nature* **1997**, *386*, 143−149.
(8) Lakes, R. *Science* **1987**, *235*, 1038−1040.
(9) (a) Furneaux, R. C.; Rigby, W. R.; Davidson, A. P. *Nature* **1989**, *337*, 147−149. (b) Searson, P. C. *Appl. Phys. Lett.* **1991**, *59*, 832−833.
(10) (a) Tonucci, R. J.; Justus, B. L.; Campillo, A. J.; Ford, C. E. *Science* **1992**, *258*, 783−785. (b) Pearson, D. H.; Tonucci, R. J. *Science* **1995**, *270*, 68−70.

10.1021/cm990195d CCC: $18.00
Published on Web 09/18/1999

track etching of polymers,[11] and excimer laser micromachining[12] can only produce porous membranes with essentially 1D channel structures. Methods based on foaming of emulsion solutions[13] and sintering of ceramic particles[14] are capable of creating 3D porous structures, but these methods have very little control over the distribution of pore size. Methods based on the assembly of block copolymers usually only form arrays of spherical pores that are isolated from each other.[15] Recent demonstrations based on replica molding against various types of templates provide a straightforward and effective route to porous materials with tightly controlled pore sizes and pore structures.[16] These templating methods, however, still have some problems—for example, most of these procedures were unable to generate free-standing porous membranes or to completely expose all pores on and within the porous materials.

We have recently demonstrated a templating procedure for fabricating 3D porous membranes from UV- (or thermally) curable organic prepolymers or sol−gel precursors to ceramic materials. As reported briefly in two papers,[17] these porous membranes have a periodic structure similar to that of an inverse opal—each of them consists of a highly ordered array of air balls that are interconnected to each other by circular "windows". Compared with porous membranes fabricated using other approaches, each membrane described in this paper exhibits the following attractive features: (i) an array of uniform, spherical pores whose size can be precisely controlled in the range from 100 nm to 10 μm by changing the size of particles; (ii) a three-dimensional interconnected network of channels in the bulk; and (iii) a hexagonal array of completely exposed, circular holes on both top and bottom surfaces of each piece of membrane film. These membranes also have a long-range, 3D periodic structure; this property makes them particularly useful as PBG materials. Some of them may even exhibit complete band gaps. This paper describes a detailed study on the fabrication and characterization of these 3D porous membranes, including comparison between different colloidal particles that serve as templates, variation of precursor materials, examination of the porous structure by scanning electron microscopy (SEM) and transmission electron microscopy (TEM), testing of mechanical strength, and measurements on the permeabilities of air and a number of solvents through one of these membranes.

Experimental Section

Materials and Substrates. Monodispersed polystyrene (PS) beads (aqueous dispersions, ≥100 nm in diameter) were obtained from Polysciences (Warrington, PA). Monodispersed colloidal particles of silica (aqueous dispersions, 100 nm−1 μm in diameter) were obtained from Nissan Chemical Industries (Tarrytown, NY) or Duke Scientific (Palo Alto, CA). All dispersions were diluted to ∼0.05% (wt) with deionized water prior to use. Ultraviolet-curable precursors to polyurethanes (NOA 60, 71, 72, 73, 88) were obtained from Norland Products (New Brunswick, NJ), and a UV-curable precursor (SK-9) to poly(acrylate−methacrylate) copolymer (PAMC) was purchased from Summers Optical (Fort Washington, PA). Sol−gel precursors to oxide ceramics—titanium(IV) isopropoxide (99.999%) and tetramethyl orthosilicate (TMOS, 98%)—were used as received from Aldrich. The glass substrates were obtained from Corning Glass Works (Corning, NY) and were washed with (in this order) acetone, 2-propanol, and a nonionic surfactant (Texclean 100 from Texwipe, Upper Saddle River, NJ), and finally rinsed with deionized water.

Fabrication of the Packing Cell. Figure 1A shows the schematic procedure that was used in the assembly of spherical particles.[18] The cell was formed from a square frame of photoresist sandwiched between two glass substrates. A two-step photolithographic procedure was used to pattern the square frame on one of the glass substrates: (i) a ∼12-μm-thick (*H*) photoresist film (Microposit 1075, Shipley, MA) was spin-coated on the substrate and then exposed to a UV light for ∼85 s through a photomask of the square frame;[19] (ii) the resist film was then exposed to the same UV source for an additional ∼8 s through another mask of parallel lines (100 μm in width and separated by 100 μm). The two masks were aligned such that the parallel lines on the second mask overlapped with at least one side of the square frame.[20] As a result, an array of trenches (h < 0.3 μm deep) was generated on this side of the frame after developing the photoresist; these trenches subsequently allowed the solvent to flow out while retaining the spherical particles. The thickness of the cell can be varied to adjust the assembled lattice of particles to a desired thickness. A small hole was formed in the top substrate (mechanically drilled or chemically etched in aqueous HF), and a glass tube was attached to this hole using an epoxy adhesive. The cell was usually assembled in a clean room and held together with binder clips.

Formation of Opaline Lattices by Self-Assembly. After injecting an aqueous dispersion of monodispersed colloidal particles into the cell (Figure 1A), a slight positive pressure of N_2 was applied through the glass tube. This pressure forced the solvent to flow through the channels. The colloidal particles were retained at the bottom of the cell and assembled into a cubic-close-packed (ccp) structure (similar to that of a natural

(11) (a) Yoshida, M.; Asano, M.; Suwa, T.; Reber, N.; Spohr, R.; Katakai, R. *Adv. Mater.* **1997**, *9*, 757−758. (b) Ballew, H. W. *Am. Biotechnol. Lab.* **1997**, *May*, 8−10.

(12) Rebhan, U.; Endert, H.; Zaal, G. *Laser Focus World* **1994**, *November*, 91−96.

(13) (a) LeMay, J. D.; Hopper, R. W.; Hrubesh, L. W.; Pekara, R. W. *MRS Bull.* **1990**, *15* (12), 19−53. (b) Even, W. R., Jr.; Gregory, D. P. *MRS Bull.* **1994**, *19* (4), 29−33.

(14) (a) Morimoto, T. *CHEMTECH* **1985**, *February*, 112−117. (b) Leenaars, A. F. M.; Keizer, K.; Burggraaf, A. J. *CHEMTECH* **1986**, *February*, 560−564.

(15) (a) Widawski, G.; Rawiso, M.; Franáois, B. *Nature* **1994**, *369*, 387−389. (b) Jenekhe, S. A.; Chen, X. L. *Science* **1999**, *283*, 372−375.

(16) (a) Davis, S. A.; Burkett, S. L.; Mendelson, N. H.; Mann, S. *Nature* **1997**, *385*, 420−423. (b) Ozin, G. A. *Acc. Chem. Res.* **1997**, *30*, 17−27. (c) Imhof, A.; Pine, D. J. *Nature* **1997**, *389*, 948−951. (d) Velev, O. D.; Jede, T. A.; Lobo, R. F.; Lenhoff, A. M. *Chem. Mater.* **1998**, *10*, 3597−3602. (e) Holland, B. T.; Blanford, C. F.; Stein, A. *Science* **1998**, *281*, 538−540. (f) Wijnhoven, J. E. G. J.; Vos, W. L. *Science* **1998**, *281*, 802−804. (g) Caruso, R. A.; Giersig, M.; Willig, F.; Antonietti, M. *Langmuir* **1998**, *14*, 6333−6336. (h) Matsushita, S. I.; Miwa, T.; Tryk, D. A.; Fujishima, A. *Langmuir* **1998**, *14*, 6441−6447. (i) Yang, P.; Deng, T.; Zhao, D.; Feng, P.; Pine, D.; Chmelka, B. F.; Whitesides, G. M.; Stucky, G. D. *Science* **1998**, *282*, 2244−2246. (j) Vlasov, Y. A.; Yao, N.; Norris, D. J. *Adv. Mater.* **1999**, *11*, 165−169. (k) Davey, R. J.; Alison, H.; Cilliers, J. J.; Garside, J. *Chem. Commun.* **1998**, 2581−2582. (l) Johnson, S. A.; Ollivier, P. J.; Mallouk, T. E. *Science* **1999**, *283*, 963−965. (m) Zakhidov, A. A.; Baughman, R. H.; Iqbal, Z.; Cui, C.; Khayrullin, I.; Dantas, S. O.; Marti, J.; Ralchenko, V. G. *Science* **1998**, *282*, 897−901. (n) Kresge, C. T.; Leonowicz, M. E.; Roth, W. J.; Vartuli, J. C.; Beck, J. S. *Nature* **1992**, *359*, 710−712. (o) Hou, Q.; Leon, R.; Petroff, P. M.; Stucky, G. D. *Science* **1995**, *268*, 1324−1327. (p) Ying, J. Y.; Mehnert, C. P.; Wong, M. S. *Angew. Chem., Int. Ed.* **1999**, *38*, 56−77.

(17) (a) Park, S. H.; Xia, Y. *Adv. Mater.* **1998**, *10*, 1045−1048. (b) Park, S. H.; Xia, Y. *Chem. Mater.* **1998**, *10*, 1745−1747.

(18) (a) Park, S. H.; Qin, D.; Xia, Y. *Adv. Mater.* **1998**, *10*, 1028−1032. (b) Park, S. H.; Xia, Y. *Langmuir* **1999**, *15*, 266−273. (c) Gates, B.; Qin, D.; Xia, Y. *Adv. Mater.* **1999**, *11*, 466−469.

(19) The exposure time has to be found out experimentally. It depends on the exact thickness of the photoresist film and the actual power of the UV light source.

(20) Channels could also be generated on all sides of the photoresist frame to increase the packing speed of particles.

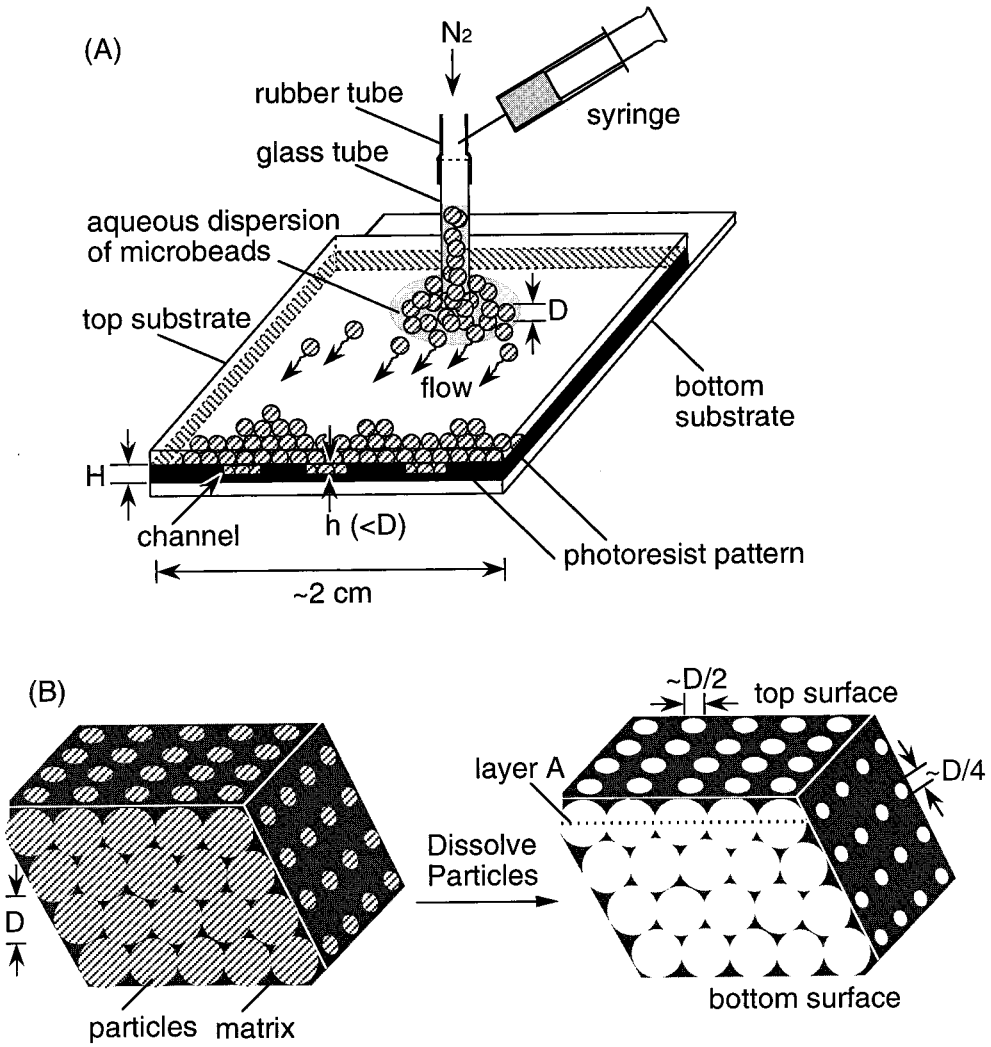

Figure 1. (A) Schematic procedure for the assembly of spherical particles into crystalline arrays. The aqueous dispersion of monodispersed particles was injected into the cell with a syringe. (B) Three-dimensional cut-away of the procedure that generates porous membranes by templating against crystalline assemblies of colloidal particles, followed by selective etching.

opal) under continuous sonication (Bransonics 1510).[21] At a given pressure of N_2 gas, the rate of packing along the direction of solvent flow decreased substantially as the particles became smaller: for example, in an ~12-μm-thick and ~2-cm-wide cell, the rate was approximately 0.1 and 0.05 mm/h for 480- and 100-nm polystyrene beads, respectively. The opaline assembly of particles was dried under ambient conditions, while the top glass substrate was still on.

Fabrication of 3D Porous Membranes. The 3D opaline arrays of colloidal particles can serve as templates for the formation of porous membranes. The void spaces among the particles could be easily filled with liquid precursors of choice, such as UV-curable organic prepolymers, alkoxide precursors to ceramic materials, or solutions of functional polymers. After solidifying the precursor, the colloidal particles were removed by selective chemical etching, leaving behind a 3D porous membrane (Figure 1B) consisting of a highly ordered architecture of interconnected spherical pores.

The UV-curable prepolymers to polyurethanes or poly(acrylate−methacrylate) copolymers employed in the membrane fabrication were used as received. Both polystyrene beads and silica colloids can be used as templates. A few drops of the liquid precursor was applied along the lower edge of the packing cell. The void spaces among the colloidal particles were filled spontaneously by capillary action. The prepolymer was cured by exposure to a broad-band UV light source (λ_{max} $\approx$ 365 nm). The colloidal particles in the crystalline array changed very little in their positions during the templating process because they were tightly confined by the packing cell. Our approach, therefore, has a unique capability that allows the formation of porous membranes with three-dimensional interconnected channel structures. After soaking the assembled cell in water, the glass plates were carefully separated, and a composite thin film containing the UV-cured polymer and colloidal particles was obtained. The polystyrene particles could be selectively dissolved by immersing the film in a toluene bath for approximately 2 h. Silica particles could be chemically etched with hydrofluoric acid (49% in water) for ~2 h, followed by rinsing with water. *CAUTION: Hydrofluoric acid (HF) is extremely corrosive and should be handled with care.* The free-standing membranes were transferred with a copper wire frame for subsequent imaging and characterization. The spherical pores within each membrane have almost the same dimension as that of the particles used to fabricate the templates.

The sol−gel precursors to oxide ceramics were also used as received. The dilution of the sol−gel precursors in an alcohol reduced their reactivities toward atmospheric moisture. In this case, only polystyrene beads can be used as templates, because the oxide ceramics are also soluble in aqueous HF solutions. The opaline assemblies were formed from polystyrene beads as previously described and dried under ambient conditions. The titania precursor solution in 2-propanol (2:5, v/v) was also injected into the crystalline structure by capillary action. The device was kept in a glovebox circulated with nitrogen gas until

(21) For a comprehensive review, see, Hench, L. L.; West, J. K. *Chem. Rev.* **1990**, *90*, 33−72.

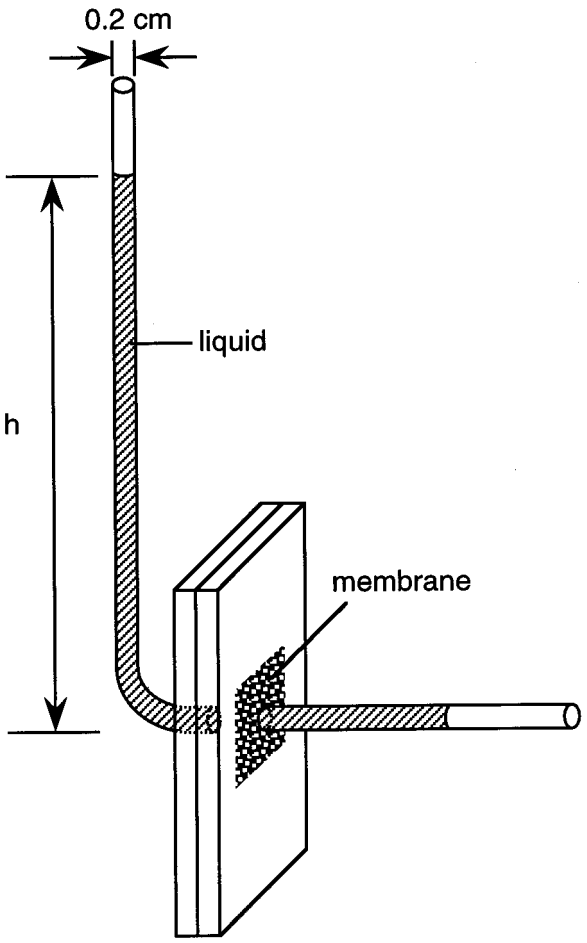

Figure 2. Schematic illustration of the flow cell used for measuring the permeability of a liquid through a polymeric membrane. A solvent flow from the left side to the right was driven by a solvent height difference between the two sides of the membrane. The porous film was held perpendicular to the solvent flow.

the opaline array of colloidal particles had been completely filled with the liquid precursor. Upon evaporation of 2-propanol, the precursor hydrolyzed to the oxide in the presence of atmospheric moisture.[21] Multiple insertions of precursor solution into the packing were used to fill the void spaces as completely as possible. The glass substrates were separated, and the resulting titania film impregnated with PS spheres was then etched as discussed in the previous section. Silica membranes were fabricated using a similar procedure that consists of precursor insertion, hydrolysis, and subsequent etching of PS particles by toluene. The concentration of the precursor solution (in methanol) was 1:1 (v/v).

Measurement of Porous Size Distribution and Permeabilities. The pore size distribution and gas permeability of the porous membrane was measured at Porous Materials, Inc. (Ithaca, NY). The liquid permeability was measured using a homemade flow cell, schematically shown in Figure 2.[22] This cell was designed with two sidearms (glass tubes), each attached to a glass slide over a circular hole ($\phi \approx 1$ mm). A piece of free-standing membrane was held between two Teflon spacers and centered over the two holes. This apparatus was held together with binder clips around the edges of the glass slides. The Teflon tape around the membrane also provided a tight sealing for this flow cell. The initial height (h_0) of liquid in the left arm drives a flow of solvent through the membrane from the left side to the right. The solvent continuously permeates through the membrane to establish a set of heights (h_t) versus time (t). The permeability (τ) for each solvent was

(22) Liu, G.; Ding, J. *Adv. Mater.* **1998**, *10*, 69−71.

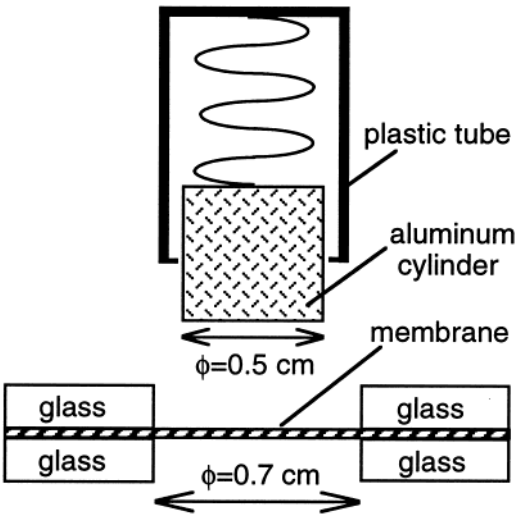

Figure 3. Schematic illustration of the device used for measuring the mechanical strength of a porous membrane.

calculated by exponentially fitting each curve (h_t versus t) with the following equation:

$$h_t = h_0 \exp(-t/\tau) \quad (1)$$

Measurement of Mechanical Strength. The mechanical strength of the membrane was tested semiquantitatively using an approach similar to the Whilhemy plate technique that is widely used to measure the surface tension of a liquid.[23] Figure 3 shows the schematic illustration of such a homemade device: the key component is an aluminum cylinder (∼0.5 cm in diameter) attached to a spring that hangs to the ceiling of a plastic tube. A piece of free-standing membrane was mounted between two glass substrates, each with an ∼0.7-cm hole in the center. After the aluminum cylinder had been brought into contact with the membrane, it was vertically pressed against the membrane with an increasing pressure until the membrane was broken. At this point, the vertical position of the aluminum cylinder relative to the end of the plastic tube was marked on the cylinder with a pen. When the device was turned over by 180 deg, objects with known weights were placed on the aluminum cylinder until the marked position was reached. The total weight of the objects and the weight of the aluminum cylinder were then used to calculate the mechanical strength of the membrane.

Other Instrumentation. The photolithography used a 3-in. aligner (Quintel-2001, Mountain View, CA). Optical images were taken with a Kodak digital camera DC-260 (Eastman Kodak, Rochester, NY). The high-resolution images of crystalline assemblies and porous membranes were obtained using a field emission scanning electron microscope (SEM, JEOL-6300F, Peabody, MA). The SEM was operated with an accelerating voltage of 15 kV. Samples prepared for SEM were sputtered with thin films of gold (<25 nm in thickness) before imaging. Because the gold was usually sputtered along the direction perpendicular to the surface of the membrane, this process should not significantly change the pore size. TEM images were obtained on a Philips 430, with an accelerating voltage of 200 kV. The samples for TEM studies were manually ground and dispersed on carbon-coated grids before imaging.

Results and Discussion

The strategy described here generates 3D porous membranes of polymers or ceramic materials by filling

(23) Johnson, R. E., Jr.; Dettre, R. H. In *Wettability*; Berg, J. C., Ed.; Marcel Dekker: New York, 1993; p 13.

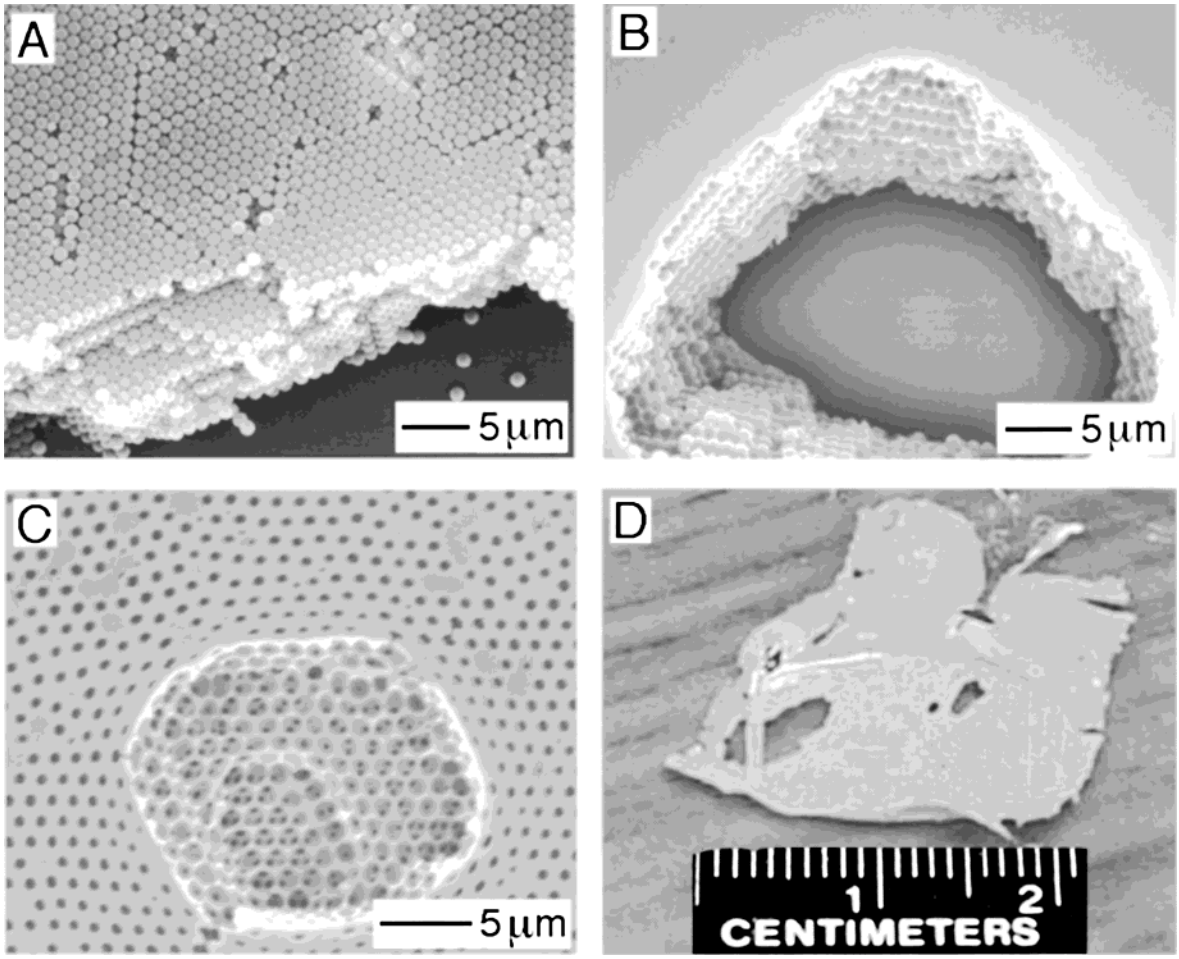

Figure 4. (A) SEM image of an opaline lattice formed from 1.05-μm PS beads. The hexagonal close-packing of the (111) face is clearly seen on this image. (B) SEM image of a composite film made of PS beads and the UV-cured polyurethane. (C) SEM image of a polyurethane membrane indicating the interconnected structure of the membrane. (D) Photograph of a piece of free-standing porous membrane that was fabricated by templating against an opaline array of 1.05-μm PS beads assembled in a ~12-μm thick cell.

the void spaces in an opaline array of colloidal particles with an appropriate precursor, followed by solidification of the precursor matrix and selective etching of the particles. This method provides a number of advantages for forming 3D porous membranes: (i) It is relatively fast. It has been shown that opaline arrays of colloidal particles can be assembled over areas as large as ~1 cm^2 in 1−2 days.[18] (ii) It provides a tight control over the thickness of the membrane, the size of pores, and the density of surface pores. The diameter of the spherical pores in the bulk can be varied in a controllable way in the range from 100 nm to 10 μm by changing the size of particles. A density of pores up to ~4.5×10^{10} per cm^2 has been achieved on the top and bottom surfaces of the membrane. (iii) It offers a simple and effective route to porous membranes consisting of a long-range periodic structure. Each membrane produced using this method contains a 3D interconnected network of air balls with a uniform size. (iv) The capability and versatility of this templating technique is further extended in the choice of materials. We have shown that membranes can be fabricated from a variety of prepolymers and sol−gel precursors to ceramic materials.

3D Porous Membranes of Organic Prepolymers. Self-assembly of spherical particles into opaline structures has been described in detail elsewhere.[18] Here we focus on the templating of these crystalline arrays to form 3D porous structures. Figure 4 shows SEM images of a crystalline array of polystyrene beads at different stages of the templating process. Figure 4A gives the SEM image of an opaline array that was formed in an ~12-μm-thick cell from 1.05-μm polystyrene beads. This crystalline assembly exhibits a ccp structure, or a face-center-cubic (fcc) lattice, with the (111) face parallel to the surfaces of the glass slides. This crystalline array was subsequently filled with a liquid prepolymer to polyurethane (see Figure 1B). Figure 4B shows an SEM image of this composite structure that consists of PS beads and polyurethane. The prepolymer had been cross-linked by exposure to the UV light. When the spherical PS beads were removed by selective etching in toluene, a free-standing 3D porous membrane was obtained (Figure 1B). Figure 4C also shows a region of the membrane where a portion of the top surface ("skin") was accidentally removed during sample preparation. This SEM image suggests a highly ordered and interconnected network of pores inside the membrane film. On the basis of the ccp model, the membrane generated by templating against an opaline assembly should have an internal porosity ≥74%. As one of the advantages over other methods, our approach is capable of creating an ordered array of circular holes on the top and bottom surfaces of the membrane. As shown in Figure 4C, the

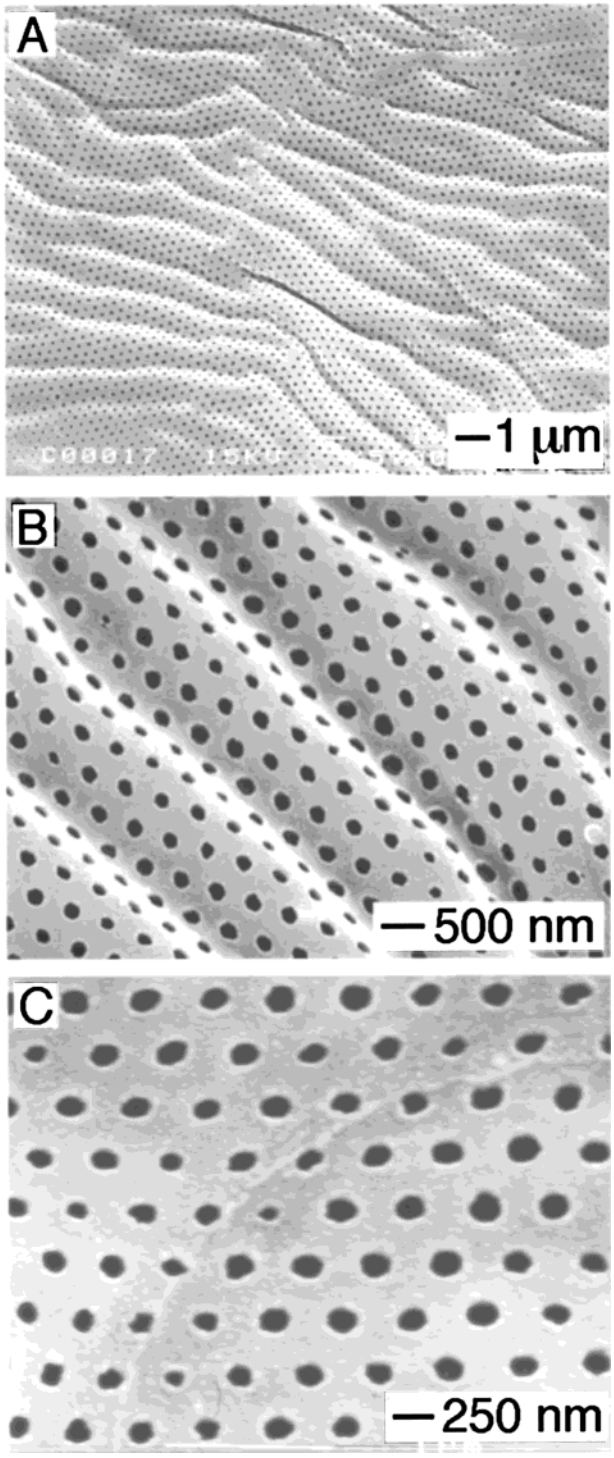

Figure 5. SEM images of a free-standing PAMC membrane that was fabricated by templating against an opaline array of 480-nm PS beads. (A) Image showing the stability of the membrane under deformation. (B, C) SEM images of the top (B) and bottom (C) surface of the membrane film, respectively. Each surface shows a similar hexagonal array of pores that ensures the accessibility of the spherical pores in the bulk.

pores on the surfaces of the membranes are ~0.5 μm in diameter and separated by ~1 μm; the air balls in the bulk are ~1 μm in size; and the circular windows connecting adjacent spherical pore are ~250 nm in dimension. Using this method, porous membranes with a uniform pore structure can be routinely fabricated over areas ≥1 cm^2 (Figure 4D). The ability to form membranes over large areas makes it possible to

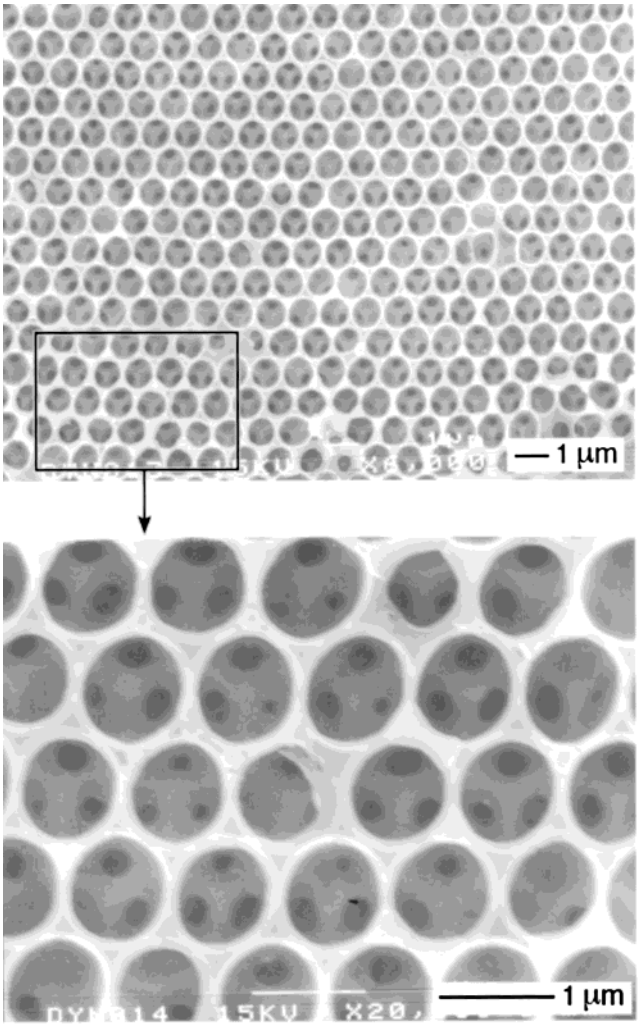

Figure 6. SEM images of a polymer membrane fabricated by templating the PAMC precursor against a crystalline assembly of 0.99-μm silica colloids. These images are a cross-sectional view of the membrane at the layer A of Figure 1B.

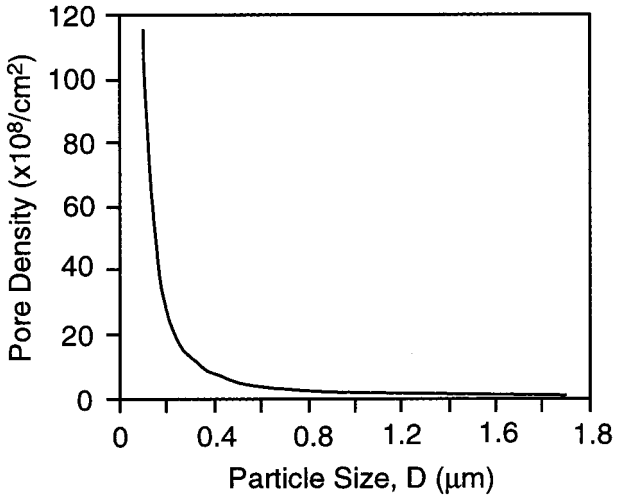

Figure 7. Relationship between the density of pores on the surfaces of the membranes and the size of particles.

incorporate these membranes into flow systems for further characterization and utilization.

We have been able to extend this technique to other polymer systems, such as poly(acrylate−methacrylate) copolymers (PAMC). Figure 5A shows the SEM image

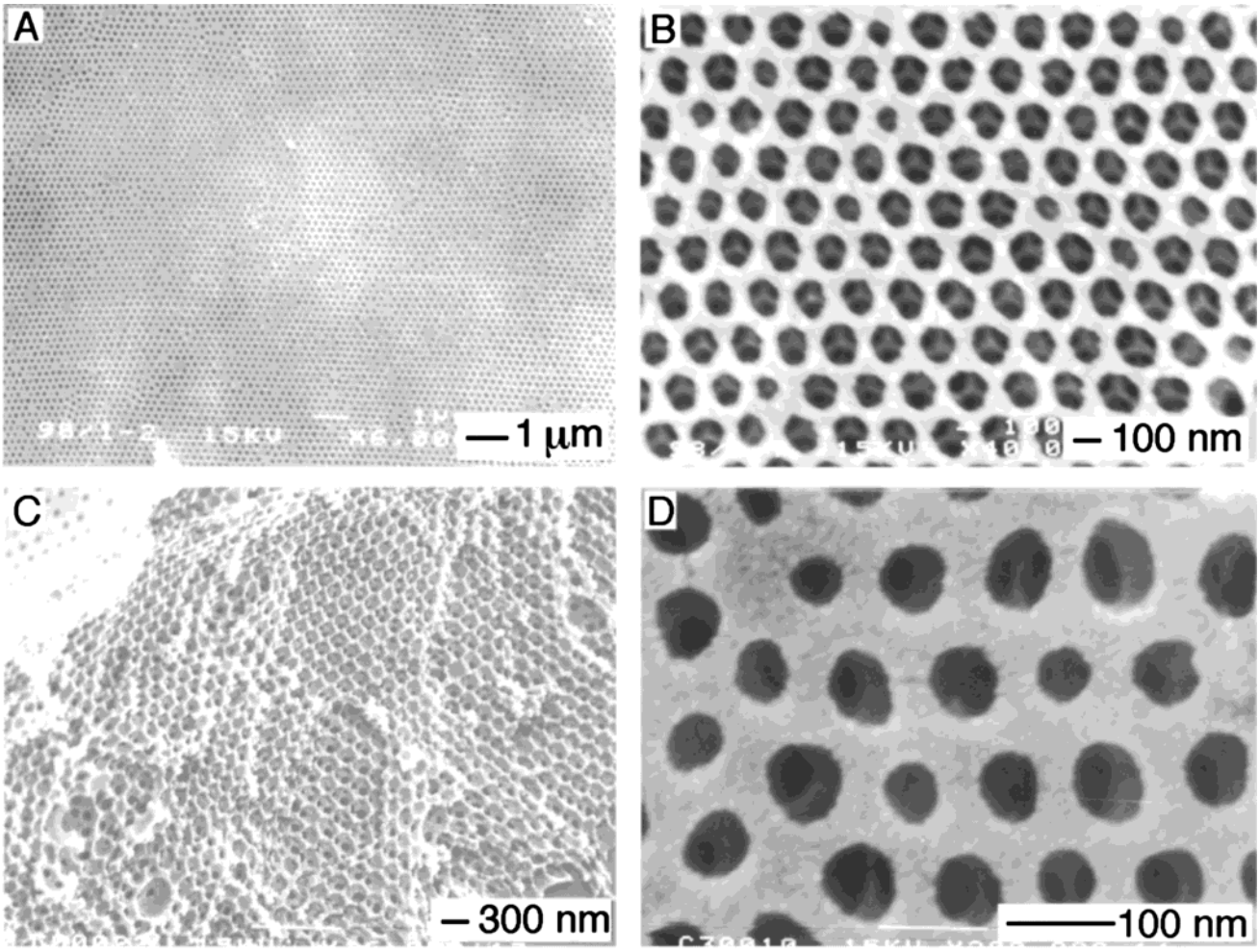

Figure 8. (A−C) SEM images of a PAMC membrane fabricated from a ccp array of 200-nm PS beads: (A, B) Top surface of the membrane with the interconnected porous structure visible through the pores. (C) Cross-sectional view of the same membrane showing a long range order in all three dimensions. (D) SEM image of the top surface of a PAMC membrane fabricated by templating against an opaline lattice of 100-nm PS beads. This membrane has a density of surface pores as high as $\sim 10^{10}/cm^2$.

of a free-standing PAMC membrane that was fabricated by templating against an opaline array of 480-nm PS beads. Ripples observed on this polymeric membrane resulted from a folding when this membrane is placed on a carbon tape for SEM imaging. This polymeric membrane was able to withstand these deformations, indicating its flexibility and relatively good mechanical strength. Figure 5B,C shows a closeup view of the top and bottom surface of this free-standing PAMC membrane, respectively. Templating against a 3D crystalline array of colloidal particles forms porous membranes with a similar hexagonal pattern of holes on both top and bottom surfaces of the membrane.

Opaline arrays of monodispersed silica colloids can also serve as templates to generate 3D porous membranes. Figure 6 shows SEM images of a PAMC membrane that was fabricated by templating against a opaline assembly of silica beads with a diameter of ~ 0.99 μm. The silica colloids were selectively removed by etching in an aqueous HF solution. These SEM images were taken from a section inside the membrane, that is, the layer A in Figure 1B. The long-range order and connection among adjacent air balls are obviously seen in these SEM images. We believe that this technique should be extendible to a variety of other colloidal particles made of different kinds of organic polymers or inorganic ceramics. The wide range of choices that we have for colloidal particles and matrix materials should allow us to fabricate porous membranes with tunable structures and properties.

Control over Pore Size and Surface Pore Density. The size and density of pores on the top and bottom surfaces of each membrane are determined by the diameter of spherical particles used as templates. We have been able to generate porous membranes from templates with particles sizes in the range from $\sim$100 nm to $\sim$10 μm. We found that the dimension of "windows" that interconnect adjacent spherical pores was approximately one-quarter of the particle size and that the diameter of holes on the membrane surfaces was approximately half of the particle size (Figure 1B). The density of pores on the membrane surface also depends on the size of particles. The technique described here allows a unique control over the density of pores that are always arranged into hexagonal arrays on the surfaces of the membrane. Figure 7 shows the relationship between the density of surface pores (per cm^2) and the diameter of the spherical particles. This control over the surface pore density is due to the hexagonal-close-packing (hcp) structure that the particles form in the plane parallel to the substrates. A hcp pattern has been observed for both top and bottom surfaces of each

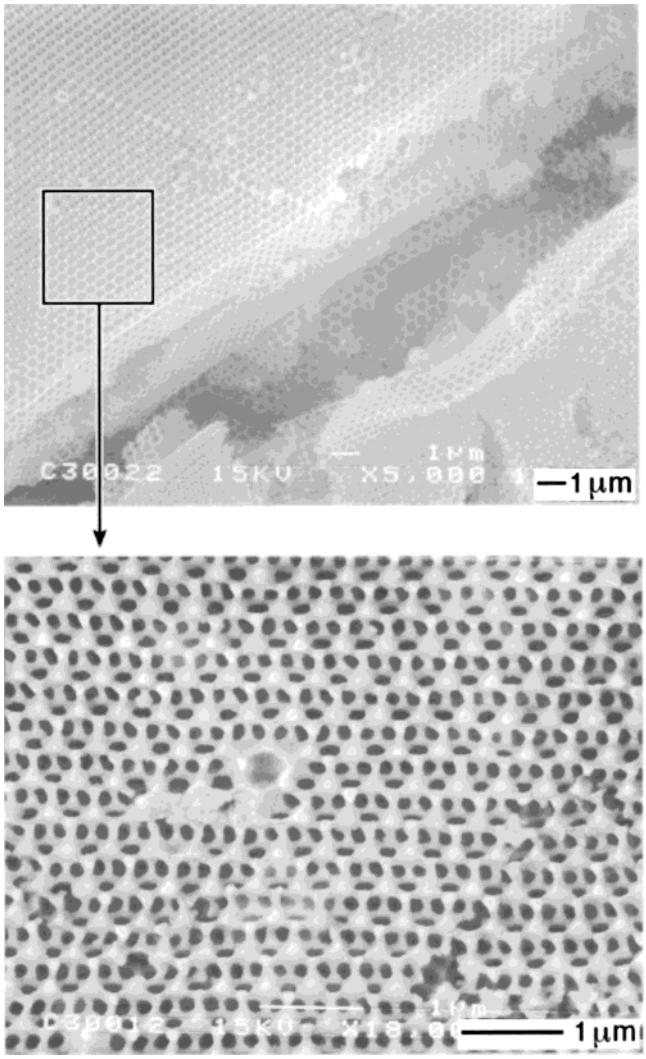

Figure 9. SEM images of a silica membrane fabricated using an array of 480-nm PS beads as the template, followed by etching of PS beads in toluene.

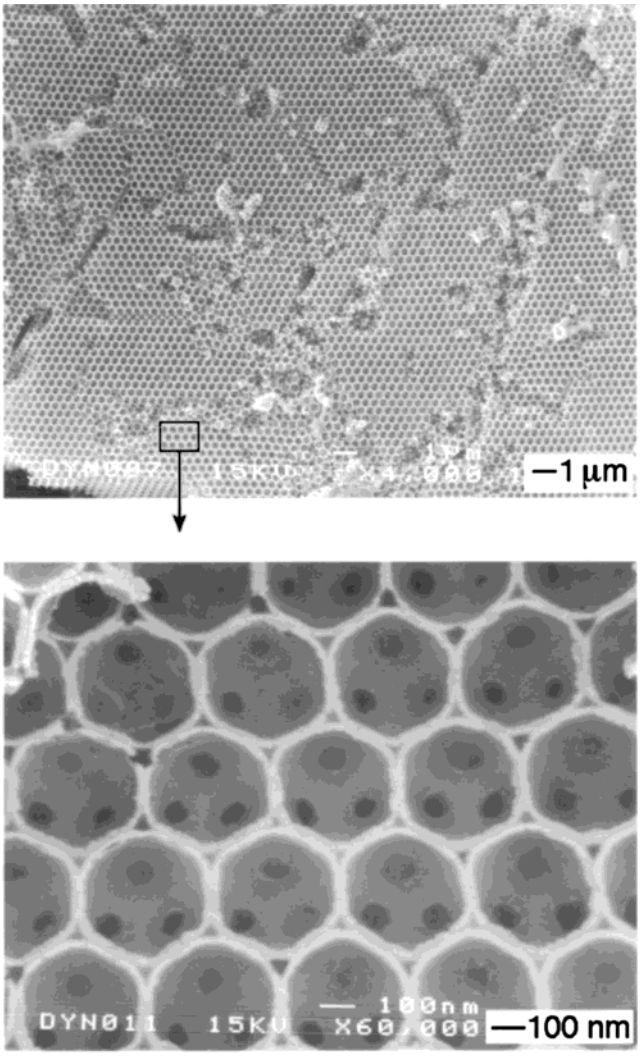

Figure 10. SEM images of a titania membrane fabricated by templating against an opaline array of 480-nm PS beads, followed by etching in toluene. The lower image shows "windows" between adjacent spherical pores resulting from a combination of the close-packing of the crystalline array and the tight confinement of the particles during templating the process.

membrane. Membranes shown in Figures 4 and 6 have a surface pore density of $\sim 10^8/cm^2$. The membrane shown in Figure 5 has a surface pore density of $\sim 4 \times 10^8/cm^2$. By templating against opaline arrays of particles with smaller sizes, it should be possible to obtain porous membranes with higher pore densities. Figure 8 shows SEM images of membranes that were fabricated by templating the PAMC precursor against opaline assemblies formed from ~200- and ~100-nm PS particles. The surface pore densities of these two membranes were $\sim 3 \times 10^9$ and $\sim 10^{10}/cm^2$, respectively. We note that the surface pore densities of membranes formed using this method are approximately a factor of 10−100 higher than those obtained by ion-track etching of polycarbonate films.[24]

3D Porous Membranes of Inorganic Ceramics. Using a similar procedure, we have also been able to fabricate ceramic membranes by templating sol−gel precursors against opaline assemblies of polymer beads. Sol−gel solutions were inserted into the void spaces around the PS particles by capillary action, and inorganic oxides were formed upon hydration of the alkoxide precursors. Titania precursors hydrated in the presence of atmospheric moisture, and the silica precursors hydrated upon immersion of the sol−gel solution into a water bath. The initial precursor completely filled the void spaces among the particles, but upon hydration and subsequent evaporation of the alcohol, the inorganic oxide became thin coatings on the spherical particles. The coating thickness increased with subsequent steps of precursor insertion and hydration. Figure 9 shows the SEM image of a silica membrane that was formed by templating against a crystalline assembly of 480-nm PS particles. The triangular void space remaining among three adjacent particles indicates the layered deposition of ceramic on the PS beads. This layered structure has also been observed on membranes fabricated with similar templating approaches.[16]

We have also fabricated titania membranes using a similar approach. Figure 10 shows the SEM image of such a membrane that was formed by templating against a crystalline array of 480-nm PS beads. These SEM images show the subsurface view of a slice cutting through the membrane, that is, layer A in Figure 1B.

(24) Corning Costar. *Nuclepore Polycarbonate Membranes, The Original!;* Cambridge, MA (1-800-492-1110).

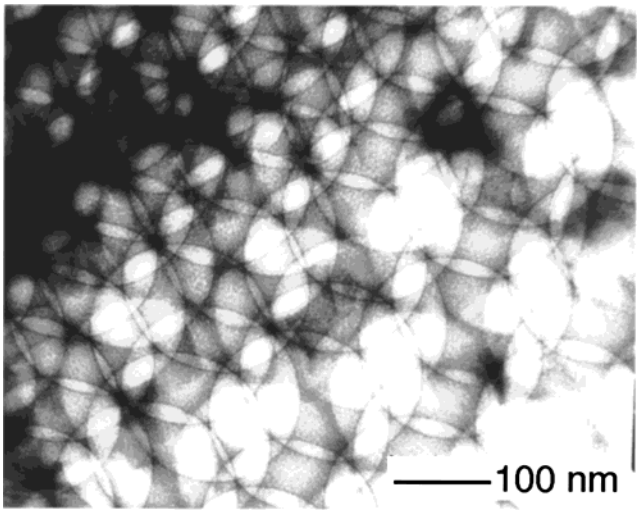

Figure 11. TEM image of a silica membrane that was fabricated by templating against an opaline array of ~200-nm PS beads.

These images clearly suggest an interconnected network of pores inside the membrane. Windows into the adjacent air balls are observed where the close-packed particles were in contact in the opaline assembly.

We also characterized the 3D porous structure of the ceramics membranes using TEM. Figure 11 gives a typical TEM image that was obtained from a silica membrane. This membrane was fabricated by templating against an opaline array of ~200-nm polystyrene beads. This image is consistent with what has been observed by SEM; it also clearly shows the interconnected character of the spherical pores. In contrast to SEM, it is impossible to distinguish the features belonging to different layers, because the formation of a TEM image is the sum of projected electrons passing through the whole sample. In addition, because the samples for TEM study were usually small grains having irregular shapes or surfaces, it is relatively difficult to obtain a TEM image showing the 3D order that is usually observed on SEM images.

Liquid Permeability of the 3D Porous Membrane. A 3D porous PAMC membrane was used as the example to measure the permeabilities of a number of solvents. This membrane was fabricated by templating the PAMC precursor against a crystalline assembly of 1.05-μm PS beads. As shown in Figure 2, the height of the solvent (h_t) in the left arm of the device was measured and plotted as a function of time. Incorporation of these membranes into a flow system provides a potentially useful experimental tool for studying the diffusion or flow of solvents through highly ordered 3D porous materials. Comparative studies are possible through control over the pore size, surface porosity, and volume of the membrane. Figure 12 shows the typical example of such a curve, which was measured for ethanol. The liquid permeability (τ) for each solvent was calculated by fitting the permeation curve (h_t versus t) with a exponential function: $h_t = h_0 \exp(-t/\tau)$.[22] Table 1 summarizes the calculated results for five commonly used solvents. A comparison between the viscosity and permeability indicates that the permeability is inversely proportional to the viscosity.

The permeation rate of a solvent through a porous membrane is determined by a number of parameters:

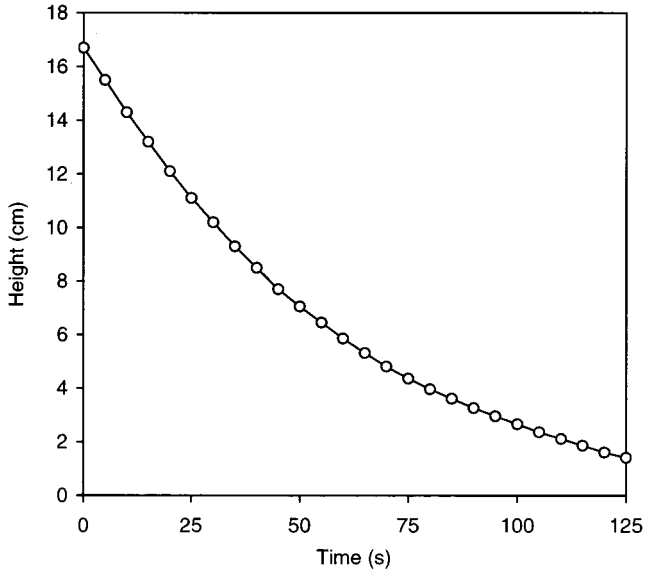

Figure 12. Permeation measurement of ethanol through a PAMC membrane. The height of ethanol in the left arm of the device was measured as a function of time. The membrane was fabricated by templating against an array of 1.05-μm PS beads. Each date point represents the average of three measurements and the solid line was obtained by an exponential fitting.

Table 1. Permeation Properties for Different Solvents[a]

liquid	viscosity, η (cP)[b]	permeability, τ (s)	transport resistance, R_m (cm^2/cP)[c]
1-butanol	2.544	1220	3.77
2-propanol	2.083	787	2.97
ethanol	1.074	440	3.22
water	0.890	283	2.50
methanol	0.544	180	2.60

[a] The area (A) of the membrane exposed to the liquid was ~0.008 cm^2. [b] The viscosity of the solvent at 25 °C. [c] The error was ±0.16.

for example, the solvent itself, the exposed area of the membrane, the pressure difference across the membrane barrier, the thickness of the membrane, the size of pores, the density of pores, and the total volume of membrane traversed by the solvent.[25] If all the parameters associated with the membrane are held constant and only the solvent varies, the permeation constant through this porous membrane should only depend on the viscosity of this solvent and the interactions between the solvent and the membrane. Transport resistance (R_m) is another parameter that is commonly used to describe the liquid permeability of a porous membrane. It is defined as the following:[2]

$$J = (\Delta P)_t / R_m \eta \qquad (2)$$

where ΔP is the pressure difference across the membrane, J is the permeate flux, and η is the viscosity of the solvent. For the measurement system used in this paper, we have $(\Delta P)_t = h_t$ and $J = -dh_t/A\, dt$ (here A is the area of the membrane). Substitution of these expressions into eq 2 leads to

$$dh_t/h_t = -(A/R_m\eta)\, dt \qquad (3)$$

Integration of eq 3 gives

$$h_t = h_0 \exp(-tA/R_m\eta) \quad (4)$$

From eqs 1 and 4, it is clear that $R_m = A\tau/\eta$. The results in Table 1 show a slight increase in the transport resistance when the solvent is changed in the order from methanol to ethanol and 1-butanol. We believe that this increase in transport resistance reflects a stronger interaction between the solvent molecules and the membrane when the length of the alkyl chain becomes longer.

Miscellaneous Measurements on the Membrane. We also characterized the porous membranes using a number of other techniques. Again, a 3D porous PAMC membrane was used as the representative example. A capillary flow test at Porous Materials, Inc. indicates that the majority of pores of this membrane are $\sim 1\ \mu$m in size, a dimension that is consistent with our SEM measurements. The permeability of this 3D porous membrane for air is $\sim 1.24 \times 10^{-3}$ mL s^{-1} cm^{-1} atm^{-1} at room temperature. In comparison, the low-density polyethylene film has a permeability of $\sim 5 \times 10^{-8}$ mL s^{-1} cm^{-1} atm^{-1} for H_2 gas.[25] Our measurement on the mechanical strength suggests that such a membrane can hold a pressure of $\sim$0.25 atm without breaking. In other words, this membrane is capable of holding an object that is approximately 4×10^5 times over the weight of the membrane, or a piece of such membrane with an area ~ 0.8 cm^2 is strong enough to support a column of water as high as $\sim$2.6 m.

Conclusions

In summary, we have demonstrated a straightforward and versatile method for generating porous membranes with a 3D periodic structure. The success of this method relies on the templating of a liquid precursor against an opaline array of colloidal particles. Subsequent solidification of the precursor and dissolution of the colloidal particles resulted in a 3D porous membrane. By changing the particle size, we could tune the pore size of these membranes over a wide range: the spherical pores in the bulk retain the size of the particle templates, while the pores on the top and bottom surfaces are approximately half of the size of the particles. The simplicity, convenience, and fidelity of this method make it particularly useful in the fabrication of membranes that will find applications as filters in adsorption, separation, diffusion, and flow systems; as supports in catalysis or tissue engineering; as tunable photonic band-gap materials; and as low-dielectric constant materials in electronic devices. A representative example of such highly porous membranes (bulk porosities $\geq$74%) was also incorporated into a flow system to measure and study the permeabilities of different liquids. So far, this templating procedure has been successfully applied to organic prepolymers and sol−gel ceramic materials. While the polymeric membranes have been made as free-standing films with areas as large as several square centimeters, the ceramic membranes are still too fragile to be released from their solid supports. One potential solution to this problem is to use sol−gel precursors with lower shrinkage or to use organic−inorganic composite precursors.

Acknowledgment. This work has been supported in part by a New Faculty Award from the Dreyfus Foundation, a subcontract from the AFOSR MURI Center (F49620-96-1-0035) at the University of Southern California, a Royalty Research Fund, and start-up funds from the University of Washington. It used Microfabrication Laboratory at the Washington Technology Center. B.G. thanks the Center for Nanotechnology for a fellowship; Dr. M. Dreja for helpful discussions; and Dr. S. H. Park, Dr. Z. Zhong, J. Wong, and J. Lynd for their technical assistance.

CM990195D

(25) Ho, W. S. W.; Sirkar, K. K. *Membrane Handbook*; Van Nostrand Reinhold: New York, 1992.